ORIGINAL RESEARCH

Chlorogenic Acid Alleviates Aβ25-35-Induced Autophagy and Cognitive Impairment via the mTOR/TFEB Signaling Pathway

Lijuan Gao [1,2,*]
Xiaoqiong Li [1,2,*]
Shi Meng [1,2,*]
Tengyun Ma [1,2]
Lihong Wan [3,*]
Shijun Xu [1,2,*]

[1]College of Pharmacy, Chengdu University of Traditional Chinese Medicine, Chengdu, Sichuan 610075, People's Republic of China; [2]Institute of Meterial Medica Integration and Transformation for Brain Disorders, Chengdu University of Traditional Chinese Medicine, Chengdu, Sichuan 610075, People's Republic of China; [3]Department of Pharmacology, West China School of Basic Medical Sciences & Forensic Medicine, Sichuan University, Chengdu, Sichuan 610041, People's Republic of China

*These authors contributed equally to this work

Correspondence: Shijun Xu
College of Pharmacy, Chengdu University of Traditional Chinese Medicine, Chengdu, Sichuan 610075, People's Republic of China
Tel +86-28-61800231
Fax +86-28-61800234
Email xushijun@cdutcm.edu.cn

Lihong Wan
Department of Pharmacology, West China School of Basic Medical Sciences & Forensic Medicine, Sichuan University, Chengdu, Sichuan 610041, People's Republic of China
Tel/Fax +86-28-85501278
Email wanlihong1976@sina.com

Purpose: Chlorogenic acid (CGA), a phenolic acid isolated from fruits and vegetables, has been established to have neuroprotective properties in relation to Alzheimer's disease (AD). However, the precise mechanism by which CGA prevents cognitive deficits in AD has not been well studied. This study aimed to explore the potential molecular mechanism of CGA action using an Aβ25-35 induced SH-SY5Y neuron injury and cogxnitive deficits model in APP/PS1 mice.

Methods: Three-month-old male APP/PS1 double transgenic mice and a human neuroblastoma cell line (SH-SY5Y) were used to assess the effects of CGA on AD in vivo and in vitro, respectively. Cognitive function in mice was measured using a Morris water maze (MWM) test. Hematoxylin and eosin, monodansylcadaverine fluorescence, LysoTracker Red (LTR), and immunofluorescence staining were used to evaluate the morphological changes in vivo and in vitro. The protein expressions of autophagy markers (LC3B-II/LC3B-I, p62/SQSTM, beclin1 and Atg5) and lysosomal-function-related markers (cathepsin D, mTOR, p-mTOR P70S6K, p-p70s6k and TFEB) were analyzed with Western blot analyses.

Results: CGA treatment significantly improved spatial memory, relieved neuron damage, and inhibited autophagy in APP/PS1 mice (P<0.05). Moreover, CGA notably suppressed autophagosome production and enhanced autophagy flux in SH-SY5Y cells induced by Aβ25-35 (P<0.05). Further analysis showed that CGA markedly promoted lysosomal activity, and this was accompanied by upregulated cathepsin D protein expression, which was induced by the mTOR/TFEB signaling pathway in APP/PS1 mice and Aβ25-35-exposed SH-SY5Y cells (P<0.05).

Conclusion: CGA treatment restored autophagic flux in the brain and alleviated cognitive impairments in APP/PS1 mice via enhanced activation of the mTOR/TFEB signaling pathway.

Keywords: autophagy, chlorogenic acid, cognitive impairment, TFEB

Introduction

Alzheimer's disease (AD) is one of the most common forms of dementia occurring in aging people and is characterized by irreversible cognitive deficits.[1] Right now, the main therapeutic approach only involves symptom relief, and this is due to a lack of understanding regarding the precise mechanism of AD. To delay the progression of AD, it is necessary to develop more effective therapeutic agents. It is well known that insoluble amyloid-β (Aβ) peptide deposition is one of the key hallmarks of AD pathology,[2] and accumulating evidences suggest that enhancement of Aβ peptide clearance is beneficial to preventing the progression of AD.[3,4]

Macroautophagy (autophagy) is a highly conserved cellular catabolic process involved in the removal of aggregated proteins, such as Aβ depositions, so as to maintain cellular homeostasis, with the generated aggregates subsequently degraded in the lysosomes.[5] Recently, numerous studies have revealed that the induction of the autophagy-lysosome pathway provides an important therapeutic strategy for Aβ peptides clearance.[6,7] Importantly, TFEB (transcription factor EB), a basic helix-loop-helix leucine zipper transcription factor, is considered a master modulator of the autophagy-lysosome pathway that serves to mediate the activation of autophagy in neurons by modulating Aβ production.[8,9] Under normal conditions, inactive TFEB locates in the cytoplasm after being phosphorylated by mTOR (mechanistic target of rapamycin kinase) at Ser142 residue.[10] p70 ribosomal protein S6 kinase (p70S6K) is the downstream target of mTOR. In contrast, dephosphorylation of TFEB at Ser142 promotes TFEB nuclear translocation and activation. Moreover, markedly decreased TFEB levels accompany lysosomal deficits, which has been observed in patients with AD and animal model.[11,12] Enhanced activation of TFEB via suppression of the mTOR pathway exhibits a significant protective effect on the clearance of abnormal toxic tau in an AD mouse model.[11]

Chlorogenic acid (CGA) is one of the most abundant phenolic acid compounds in fruits and vegetables, including coffee and tea.[13] Currently, increasing evidences have demonstrated that CGA can be used to treat various central nervous system (CNS) diseases due to its anti-inflammatory, antioxidant and neuroprotective effects and such disorders include depression,[14] neurodegenerative disorders,[15] and alcohol-induced neuron damage.[16] Importantly, Ishida recently indicated that CGA from coffee could be used to prevent cognitive deficits and reduce Aβ plaque deposition in APP/PS1 mice.[17] However, the precise mechanism by which CGA prevent cognitive deficits in AD has not yet been elucidated. Interestingly, some evidence has shown that CGA plays a key role in the suppression of oxidative stress, inflammation, and autophagy associated with kidney injury and nonalcoholic fatty liver.[18,19] Therefore, in this current study, APP/PS1 double transgenic mice were used to evaluate whether CGA could restore brain autophagic flux and prevent cognitive impairments in mice via enhanced activation of TFEB.

Materials and Methods
Materials
Chlorogenic acid (CGA, purify≥98% by HPLC) was purchased from Baoji Herbest Bio-Tech Co.,Ltd. (Hebei, China). The Aβ$_{25-35}$ peptide (purify≥98% by HPLC) was purchased from GL Biochem (Shanghai, China) and incubated at 4°C in PBS for 1 week to form oligomeric Aβ$_{25-35}$, according to a previous publication.[20]

Methods
Cell Culture
The Human neuroblastoma cell line (SH-SY5Y) donated by National experimental cell resource sharing platform (Beijing, China) was cultured in high glucose Dulbecco's modified Eagle's medium (DMEM) (Harry Biotech, Chengdu, China) supplemented with 10% fetal bovine serum (FBS; Gibco, Grand Island, NY, USA) and 1% penicillin/streptomycin (Gibco) and incubated at 37°C in a humidified atmosphere of 5%CO_2.

Cell Viability Assay
Cell viability was measured with MTT assay. Briefly, SH-SY5Y cells were seeded into 96-well plates at a density of $3×10^3$ cells/well overnight at 37°C. Then, the cells were treated with Aβ$_{25-35}$ (20 μM) for 24 or 48h in the presence or absence of CGA (3.125, 6.25, 12.5, 25, or 50μM). Then, the culture medium was removed, and the cells were incubated for 4 h at 37°C in MTT (Sigma-Aldrich, St. Louis, MO, USA). The absorbance of the formazan was determined at 570 nm using a microplate reader (Thermo Labsystems, Franklin,MA, USA). The cell viability was expressed as follows: Cell viability=(OD$_{drug}$-OD$_{zero}$)/(OD$_{vehicle}$-OD$_{zero}$) ×100%. All of the absorption values were calculated by averaging the results of each sample in triplicate.

Animals and Drug Administration
Sixteen 3-month-old male APPswe/PS1dE9 (APP/PS1) double transgenic mice with a C57BL/6J background, weighing 25±2 g, and eight male wild-type (WT) littermates were purchased from Beijing HFK Bioscience Co., Ltd. (Beijing, China; Certificate SCXK Jing 2009–0004). All of the mice were housed in SPF conditions at 25±2°C with a 12h light/dark cycle and free access to food and water. Then the APP/PS1 or WT mice received saline or CGA (40 mg/kg) by daily oral gavage, which was administrated in a preventive mode for six months. All of the animal procedures were approved by the Institute of Meterial Medica Integration and Transformation for Brain Disorders (Chengdu, China) and performed according to the protocols of the Chengdu University of Traditional Chinese Medicine (Chengdu, China).

The APP/PS1 mice were randomly divided into two groups (n=8 in each group): AD model group and CGA treatment group. All of the mice from each group received saline or CGA (40 mg/kg) by daily oral gavage for 180 days, as based on previous studies.[21] WT mice served as the control group and were treated with an equal volume of sterile saline.

Morris Water Maze (MWM) Test

The procedure was performed as previously described.[22] The mice were trained in a 100-cm diameter circular pool filled with opaque water (30 cm deep, 22–24°C). An 8-cm transparent platform was placed 1 cm below the surface in the middle of the northeast quadrant. For the place navigation task, mice were trained for 5 days consecutively. All the tests were replicated at least twice during the period of drug treatment, while the escape latency and total swimming distance were recorded in one 60 sec session. Twenty-four hours after the end of the navigation trial, a probe test was performed with the platform removed. The time spent in the target quadrant and the numbers of plat-form-site crossovers within 60 s were recorded.

Monodansylcadaverine (MDC) Fluorescence Staining

SH-SY5Y cells were treated with $A\beta_{25-35}$ (20 μM) in the presence or absence of a 24h incubation with CGA (6.25, 12.5, 25, or 50 μM). After a 24h incubation, the cells were fixed and incubated with MDC (25 Mm; Sigma) for 30 min in 37°C. Autophagic vesicles were observed using a fluorescence microscopy (Leica Microsystems, Wetzlar, German) at an excitation wavelength of 380 nm and an emission filter of 530 nm. The MDC mean fluorescence intensity was measured using Image ProPlus software (Version 6.0, Media Cybernetics, Bethesda, FL, USA).

Transfection of mCherry GFP LC3 Adenovirus

SH-SY5Y cells were grown in 24-well plates, transfected with the mCherry-GFP-LC3 adenovirus (MOI=3), and incubated at 37°C for 24h after reaching 70–80% confluence. Then the puncta were visualized using a confocal fluorescence microscopy (Olympus, Tokyo, Japan).

Preparation of Total Protein and Nuclear Extracts

Total protein was extracted from the cells or brains of mice for use in Western blot analysis. Nuclear extraction was conducted using a Nuclear and Cytoplasmic Extraction Reagents kit, according to the manufacturer's instructions (Beyotime Biotechnology, Shang Hai,China).

Western Blot Analysis

Equal amounts of protein (30 μg) extracted from the cells or brain tissues were separated using 8%-15%SDS-PAGE gels and transferred to PVDF membranes (Millipore; Germany). Then, the membranes were blocked with 5% BSA for 1h and incubated with primary antibodies overnight at 4°C, followed by HRP-conjugated secondary antibody for 2h at room temperature. Primary antibodies against the following proteins were from Cell Signaling Technology, (Beverly, MA, USA): anti-SQSTM1/p62 (no.8025T), anti-Phospho-mTOR (no.5536T), anti-TFEB (no.37785S), anti-mTOR (no.2983S). Anti-LC3B (no. A9A503500321), anti-p70S6K (no. A9A373640725), anti-Phospho-p70S6K (no. A9A303700725), anti-β-actin (no.61A00848) were purchased from MultiSciences (Zhejiang Province, China). Anti-Beclin1 (no. AH11208656) and anti-ATG5/APG5L (no. AB04011456,) were purchased from Bioss (Woburn, MA, USA). Anti-GAPDH (no.LS191936) and anti-Cathepsin D (no.050818190315) were purchased from Servicebio (Wuhan, China) and Beyotime Biotechnology (Jiangsu, China), respectively. The membranes were visualized using an ECL kit (4A Biotech, Beijing, China) and a chemiluminescence instrument. The integrated optical density (IOD) was measured using the Image Pro Plus software (Version 6.0; Media Cybernetics), and GAPDH, β-actin or LaminA/C was used to normalize protein loading.

LysoTracker Red (LTR) Staining

Lysosomal staining was performed using LTR. After 24h of treatment with CGA (50 μM), $A\beta_{25-35}$ (20μM) was added. The other groups were added with Earle's Balanced Salt Solution (EBSS; Beyotime Biotechnology), Chloroquine (CQ; 25 μM; Meilun, Tianjin,China) and CGA (50μM) respectively. The cells were subsequently incubated with LTR (5μM) for 30 min at 37 °C, washed with PBS, and examined via fluorescence microscopy (Leica). The mean fluorescence intensity was measured using Image ProPlus software (Version 6.0; Media Cybernetics).

Confocal Immunofluorescence Staining of TFEB

Localization of TFEB was examined with immunofluorescence staining. Briefly, treated cells were fixed with 4% paraformaldehyde in PBS for 30 min at 4°C and then incubated with TFEB goat polyclone primary antibody in a 1:100 dilution overnight at 4°C. This was followed by incubation with a FITC-labeled donkey anti-goat IgG at a 1:500 dilution for 1h at the room temperature. The nucleus was stained with DAPI for 5 min. The cells were examined using a confocal microscope (Fluoview FV1000; Olympus, Tokyo, Japan), and representative cells were selected and photographed.

Transmission Electron Microscope (TEM)

The brain samples were cut into pieces ($1 \times 1 \times 1$ mm) and fixed in 2.5% (v/v, PH=7.4) glutaraldehyde-polyoxymethylene solution for 24h at 4°C. The tissues were then washed and postfixed in 2% osmium tetroxide for 2h at 4°C and embedded in Araldite Epon-81 after dehydration in ascending grades of ethanol. Ultrathin sections were cut and stained with alkaline and lead citrate uranyl acetate for 15min. The sections were examined under a transmission electron microscope (JEM-2100F, Hitachi, Japan).

Hematoxylin and Eosin (H&E) Staining

The tissues were fixed with 4% PA, they were dehydrated with gradient ethanol and xylene until they were transparent, and embedded in paraffin. Paraffin sections (4mm) were stained with hematoxylin and eosin (H&E). The staining was followed by dehydrating the tissue with ethanol, washing the tissue with xylene, and covering the slide. Finally, the slide was observed with microscope (DM1000, Leica, Germany).

Immunohistochemical Staining

Tissues were fixed with 4% paraformaldehyde (PFA) and the brains were placed in PFA overnight. Then embedded in paraffin before cutting into 4 μm sections. After pretreatment with 3% H2O2 for 15 min to quench endogenous peroxidase activity. The sections were blocked with 5% goat serum and then incubated with β-Amyloid Mouse mAb (1:100; Lot: 15126; Cell Signaling Technology,Beverly, MA, USA) as the primary antibody overnight at 4°C. A horseradish peroxidase-conjugated goat anti-rabbit IgG antibody (dilution, 1: 500) was incubated as the secondary antibody for 1 hour at room temperature after the sections were washed with PBS. The sections were washed with PBS and visualized by the DAB chromogen solution for a few seconds,dehydrated, permeabilized, and sealed. The representative images were captured using microscope (DM1000, Leica, Germany). The extent of the amyloid plaques was analyzed with Image Pro Plus software (Version 6.0; Media Cybernetics)

Statistics

All values were expressed as mean ± SEM, and $P<0.05$ was considered statistically significant. The escape latency was analyzed via one-way analysis of variance (ANOVA) with a repeated-measure factor of sessions (number of days) followed by the least significant difference testing. Other data were analyzed via one-way ANOVA with Bonferroni correction using GraphPad Prism software (Version 5; GraphPad Software, La Jolla, CA, USA).

Results

Chlorogenic Acid (CGA) Ameliorates Cognitive Deficits and Neuronal Damage

To confirm the effect of CGA on cognitive deficits and neuron damage in mice, we first evaluated the spatial memory function with MWM test. As shown in Figure 1A, there were significant differences in the escape latency among the mice of the three groups ($F_{(4, 16)} =28.59$, $P<0.0001$). The APP/PS1 mice slowly arrived at the location of the platform and exhibited a longer escape latency compared with WT mice ($P<0.01$). Moreover, the APP/PS1 mice also spent a shorter amount of time in the target quadrant ($P<0.05$, Figure 1B and D), although no significant differences in crossing time were noted, compared with WT mice ($P>0.05$, Figure 1C). Notably, CGA-treaded mice exhibited remarkable improvements in spatial memory compared with the APP/PS1 mice, which was characterized as a notable decrease in escape latency ($P<0.01$, Figure 1A) and extension of the time in the target quadrant ($P<0.05$, Figure 1B and D).

To further determine the effect of CGA on morphological changes of neurons damage, we assessed the cell morphology and number of hippocampal CA1 neurons in these mice. As shown in Figure 1E, the microstructure of Hippocampal Neuron Cells was observed and investigated by means of TEM. Electron micrographs showed that there was substantial organelle dissolution (middle panel) with high electronic-dense material deposition (lower panel) in the cytoplasm of the neurons in the APP/PS1 mice, and demyelination characteristics (upper panel). And these occurrences were absent in the mice treated with CGA. Moreover, morphological changes in hippocampal CA1 were observed after hematoxylin and eosin (H&E) staining. As shown in Figure 1F (upper panel), severe neuronal damage in the hippocampus of APP/PS1 mice was apparent, especially in CA1, with more nuclear pyknosis, nucleolus disappearance, and triangulated neuronal bodies than in WT mice. Moreover, APP/PS1 mice had significantly lower cell counts in the CA1 areas.

CGA Inhibits Aβ$_{25-35}$-Induced Autophagy in SH-SY5Y Cells

First, we determined the optimal concentration of Aβ25-35-injured cells and the safe concentration of CGA. The SH-SY5Y cells were treated with Aβ25-35 of different concentrations for 12, 24 and 36 hours to determine the optimal concentration, cell viability was detected by MTT assay. The different concentrations of Aβ$_{25-35}$
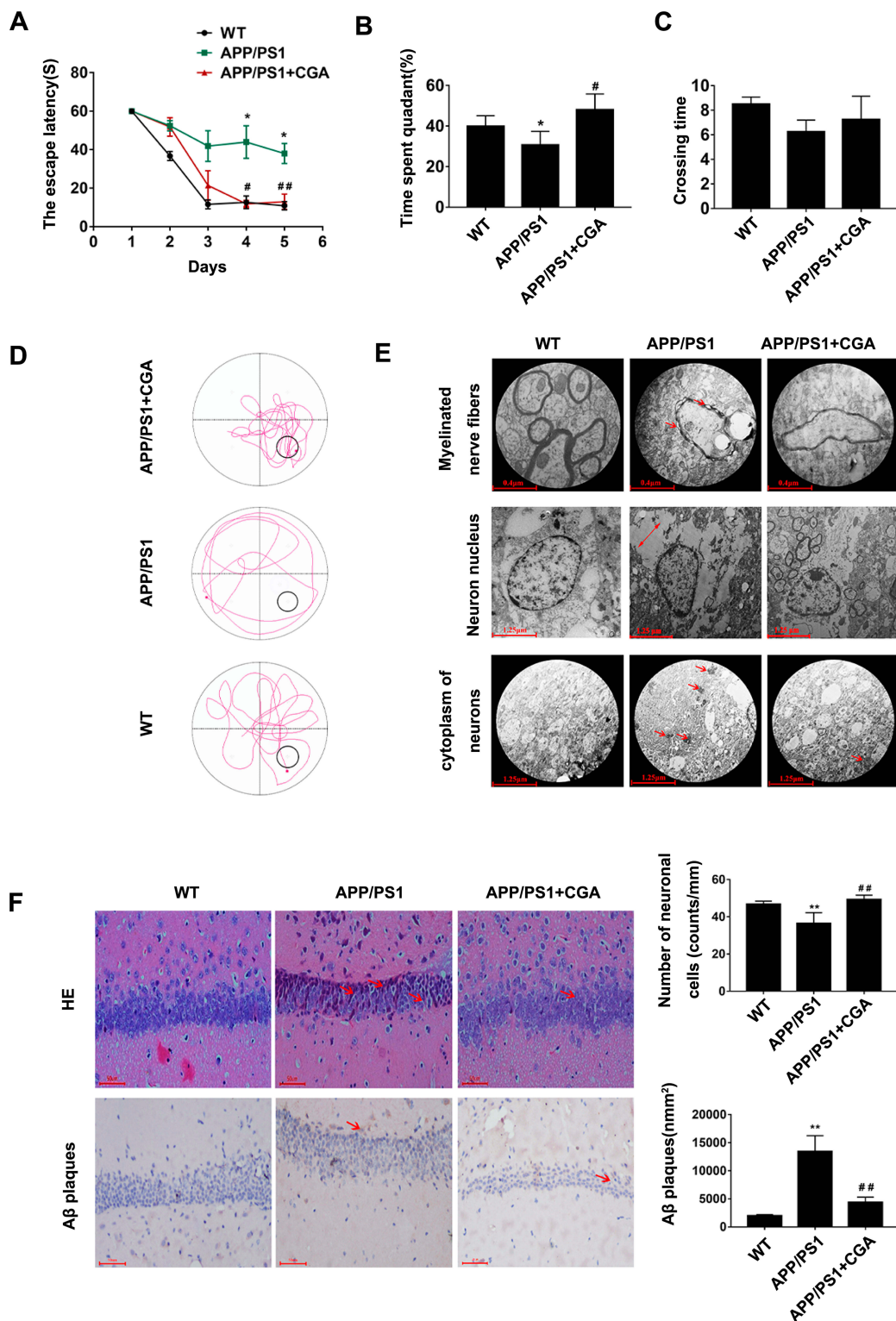
Figure 1 CGA alleviated spatial memory impairment in APP/PS1 mice and Aβ$_{25-35}$- induced neuron damage in SH-SY5Y cells.
Notes: (**A**) The escape latency of mice. (**B**) The percentage of time spent in the target quadrant. (**C**) The crossing times. (**D**) Representative swimming trajectories of the mice on the fifth trial day. (**E**) Electron micrograph of neurons in the hippocampal CA1 area of the mice.1) Myelinated nerve fibers (upper panel, arrowheads represent the Demyelination characteristics). 2) Neuron nucleus (middle panel, two-way arrows represent the intercellular space). 3) cytoplasm of neurons (lower panel, arrowheads represent the high electronic density materials). (**F**) Representative H&E stained neurons in the hippocampal CA1 area of the mice (upper panel, arrowheads represent the nuclear pyknosis), and immunohisto-chemical staining results of Aβ plaques (lower panel, arrowheads represent the Aβ plaques). Data are expressed the mean ± s.e.m for eight samples per treatment group. *P<0.05, **P<0.01 compared with the WT group or the no Aβ$_{25-35}$-treatment group; #P<0.05, ##P<0.05 compared with the APP/PS1 group or Aβ$_{25-35}$-treatment group.
Abbreviations: CGA, chlorogenic acid; AD, Alzheimer's disease; LTR, LysoTracker Red.

(5,10,20,40,80μM) induced significantly different cell viability when compared with the normal group (Fig. S A). Treatment with Aβ25-35 decreased the cell viability in a dose- and time-dependent manner. At 20μM and 24h, Aβ25-35 stably reduced the cell viability without excessive cell damage (p<0.05, Fig. S A). As such, subsequent experiments used 20μM Aβ25-35 for 24h as the optimal damage conditions. However, CGA treatment significantly decreased cell viability and showed drug toxicity at concentrations of 200-400μM at 24h (p<0.05, Fig. S B). As such, 6.26,12.5, 25,50μM were regarded as the optimum concentration range for LGT assessment in this study. To investigate the neuroprotective effect of CGA on $A\beta_{25-35}$-induced neuronal damage in SH-SY5Y cells, MTT assays were used for viability assessments. The cells were pretreated with CGA (3.125, 6.25, 12.5, 25, or 50 μM) and then treated with $A\beta_{25-35}$ (20 μM) for 24 or 48h to assess for potential neuroprotective effects. The dosages of CGA were based on our preliminary experiments, and all the doses were determined to be safe (data not shown). In order to further confirm that the dose of CGA is safe, SH-SY5Y cells were given 50 μM CGA alone. The activity of the SH-SY5Y cells was not reduced after exposure to 50μM CGA (P>0.05). Together, these results indicated that CGA had a significant protective effect in regard to cognitive deficits and neuron injury (Figure 2A). As shown in Figure 2A, CGA demonstrated a significant protective effects towards $A\beta_{25-35}$-induced neuronal damage in SH-SY5Y cells in a dose-dependent manner (P<0.05). Together, these results indicated that CGA had a significant protective effect towards cognitive deficits and neuronal injury. Next, autophagy vesicles in SH-SY5Y cells were detected using the MDC method. The data showed that $A\beta_{25-35}$ exposure significantly activated autophagic processes in SH-SY5Y cells, as evidenced by the increased fluorescent density (P<0.05, Figure 2B). In contrast, CGA treatment at a dose of 50 μM for 24h notably inhibited the increased fluorescent density resulting from $A\beta_{25-35}$ exposure (P<0.05, Figure 2B), while the fluorescent density was not altered when compared to control group (non $A\beta_{25-35}$ exposure cells). Consistent with this, Western blot analysis of LC3B-II/LC3B-I and p62/SQSTM also indicated that $A\beta_{25-35}$ exposure significantly induced the conversion of LC3B-I into LC3B-II and upregulated p62/SQSTM protein level (an autophagy substrate), which were markedly suppressed following CGA treatment (P<0.05, Figure 2C).

To further assess the influence of CGA on autophagy regulation, Western blot analysis and mCherry-GFP-LC3 virus transfection were used to measure the protein level of beclin1 and Atg5 (an autophagosome production marker) and fusion of autophagosomes with lysosomes, respectively. Clearly, $A\beta_{25-35}$ exposure significantly elevated the protein expression levels of beclin1 and Atg5, which were decreased by CGA treatment (P<0.05, Figure 2D), indicating that CGA could suppress the

production of autophagosomes. Moreover, SH-SY5Y cells stably expressing mCherry-GFP-LC3 treated with CGA showed significantly increased autolysosome, whereas autophagosome was increased in cells not treated with CGA (P<0.05, Figure 2E), suggesting that CGA could enhanced the fusion of autophagosomes with lysosomes in $A\beta_{25-35}$-exposed SH-SY5Y cells.

CGA Enhances Lysosomal Activity in SH-SY5Y Cells via the mTOR/TFEB Signaling Pathway

The observation that CGA led to the enhancement of autophagic flux prompted us to investigate whether CGA could modulate lysosomal function. The acidic intracellular compartments (lysosomes) in SH-SY5Y cells were first measured using LTR. As shown in Figure 3A, $A\beta_{25-35}$ exposure at a dose of 20 μM markedly reduced the fluorescence signal (P<0.05), indicating a reduction in intracellular acidic components resulting from $A\beta_{25-35}$ exposure. As expected, treatment with CGA (50 μM) significantly increased the LTR fluorescence (P<0.01). Next, we investigated the effect of CGA on cathepsin D, an aspartyl protease important for lysosomal proteolysis, via Western blot analysis and found profound decreased protein levels of cathepsin D in $A\beta_{25-35}$-exposed cell (P<0.01, Figure 3B). In contrast, the expression of the cathepsin D protein was significantly elevated after CGA treatment when compared with $A\beta_{25-35}$-exposed cells (P<0.01, Figure 3B), suggesting that CGA augments lysosomal functionality in SH-SY5Y cells.

Given the central role of mTOR/TFEB in the regulation of lysosome biogenesis, we next determined whether this signaling pathway was involved in CGA-induced restoration of lysosome function in $A\beta_{25-35}$-exposed SH-SY5Y cells. First, p-p70s6k/p70s6k and p-mTOR/mTOR were used to evaluate the activity of mTOR, and the data showed that $A\beta_{25-35}$ exposure demonstrated a significant activation of mTOR and this activation could be alleviated with treatment with CGA (P<0.01, Figure 3B). Moreover, it was demonstrated that $A\beta_{25-35}$ exposure suppressed TFEB nuclear translocation (Figure 3C) and significant decreased TFEB protein levels in the nucleus (P<0.01, Figure 3D). Importantly, CGA also notably restored TFEB protein levels and nuclear translocation in SH-SY5Y cells (P<0.01, Figure 3D). Moreover, CGA enhanced lysosomal activity in SH-SY5Y cells via an enhancement of TFEB translocation to the nucleus conferred by the inhibition of the mTOR pathway.
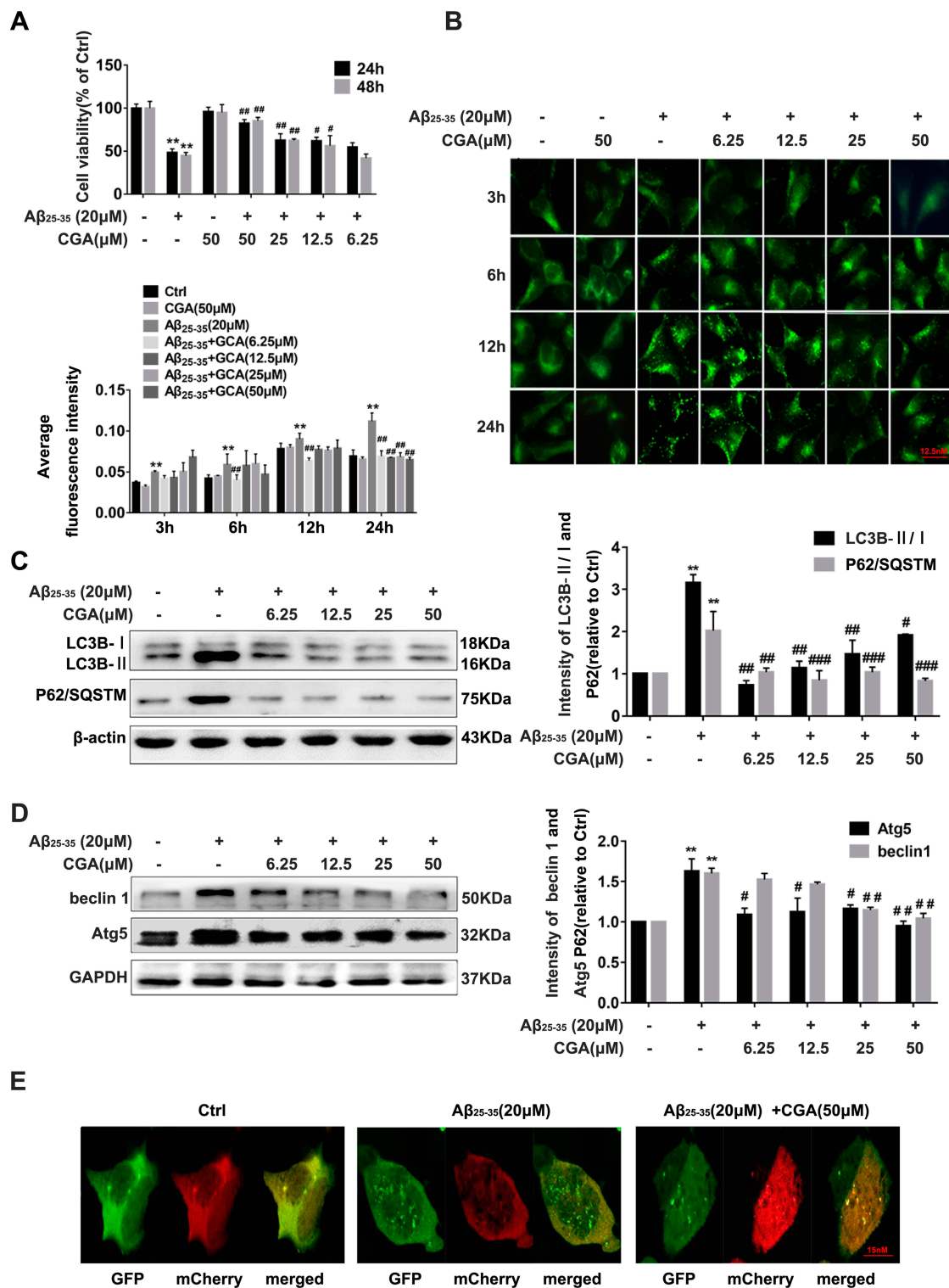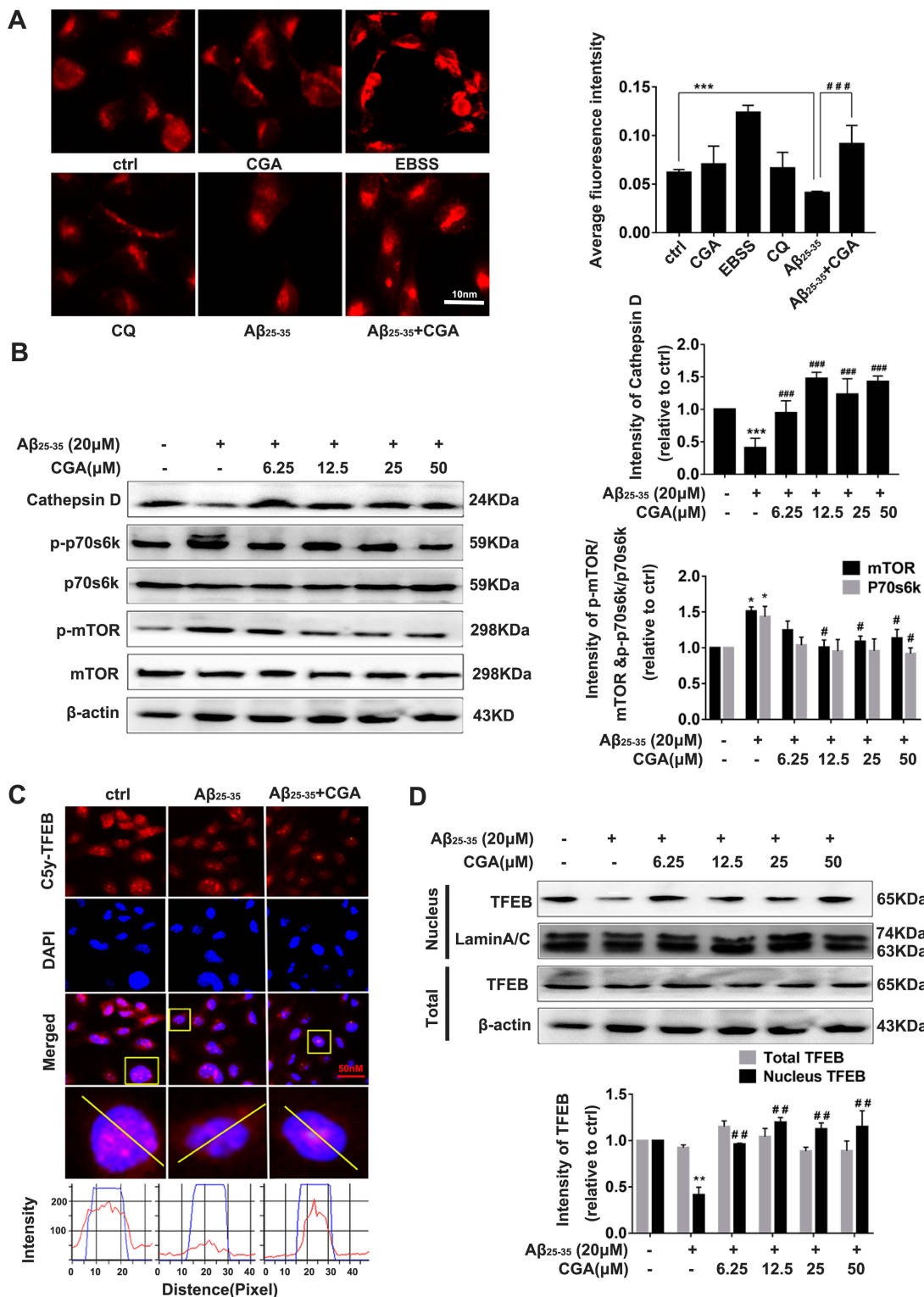
Figure 2 CGA inhibits Aβ₂₅₋₃₅-induced autophagy in SH-SY5Y cells.

Notes: (**A**) The viability of cells treated with various concentrations of CGA for 24 and 48 h was determined with MTT assay. (**B**) Representative MDC-stained autophagy vesicles in SH-SY5Y cells (right panel, ×200), and analysis of mean fluorescence intensity (left panel). (**C**) Representative Western blot imagines of LC3B-II/LC3B-I (16/18 KDa) and p62/SQSTM (75 KDa) in SH-SY5Y cells (left panel); β-actin (43 KDa) was used as a control for protein loading. The right panel shows the relative optical density values of LC3B-II/LC3B-I and p62/SQSTM between the experimental groups. (**D**) Representative Western blot imagines of beclin1 (50 KDa) and Atg5 (32 KDa) in SH-SY5Y cells (left panel); GAPDH (37 KDa) was used as a control for protein loading. The right panel shows the relative optical density values of beclin1 and Atg5 between the experimental groups. (**E**) SH-SY5Y cells expressing mCherry-GFP-LC3 stably were treated in the presence or absence of CGA. Autophagosomes (yellow foci) and autophagic flux (red-only foci) were measured with confocal fluorescence microscopy (FV1200; Olympus, Tokyo, Japan). Three independent experiments were performed, and the date are expressed the mean ± s.e.m for five samples per treatment group. **P<0.01 compared with the no Aβ₂₅₋₃₅ treatment group; #P<0.05, ##P<0.05, ###P<0.001 compared with the Aβ₂₅₋₃₅ treatment group.

Figure 3 CGA enhances lysosomal activity in SH-SY5Y cell via the mTOR/TFEB signaling pathway.

Notes: (**A**) Lysosomes were labeled with LTR and observed by fluorescence microscopy (Scale bar, 10 μm). (**B**) Representative Western blot imagines of cathepsin D (24 KDa), p70s6k (59 KDa), P-p70s6k (59 KDa), mTOR (298 KDa) and p-mTOR (298 KDa) in SH-SY5Y cells (left panel); β-actin (43 KDa) were used as a control for protein loading. The right panel shows the relative optical density values of cathepsin D, p70s6k, P-p70s6k, mTOR and p-mTOR between the experimental groups. (**C**) Immunofluorescence staining of TFEB (red) was visualized with confocal microscopy. The nucleus was stained with DAPI (Scale bar, 50 μm). (**D**) Representative Western blot imagines of TFEB (65 KDa) indicating nuclear and total protein (left panel); Lamin A/C (74/63 KDa) or β-actin (43 KDa) was used as a control for protein loading. The right panel shows the relative optical density values of TFEB between the experimental groups. Data are expressed as the mean ± s.e.m for five samples per treatment group. *P<0.05, **P<0.01, ***P<0.001 compared with no Aβ25-35 treatment group; #P<0.05, ##P<0.01, ###P<0.01 compared with Aβ25-35 treatment group.
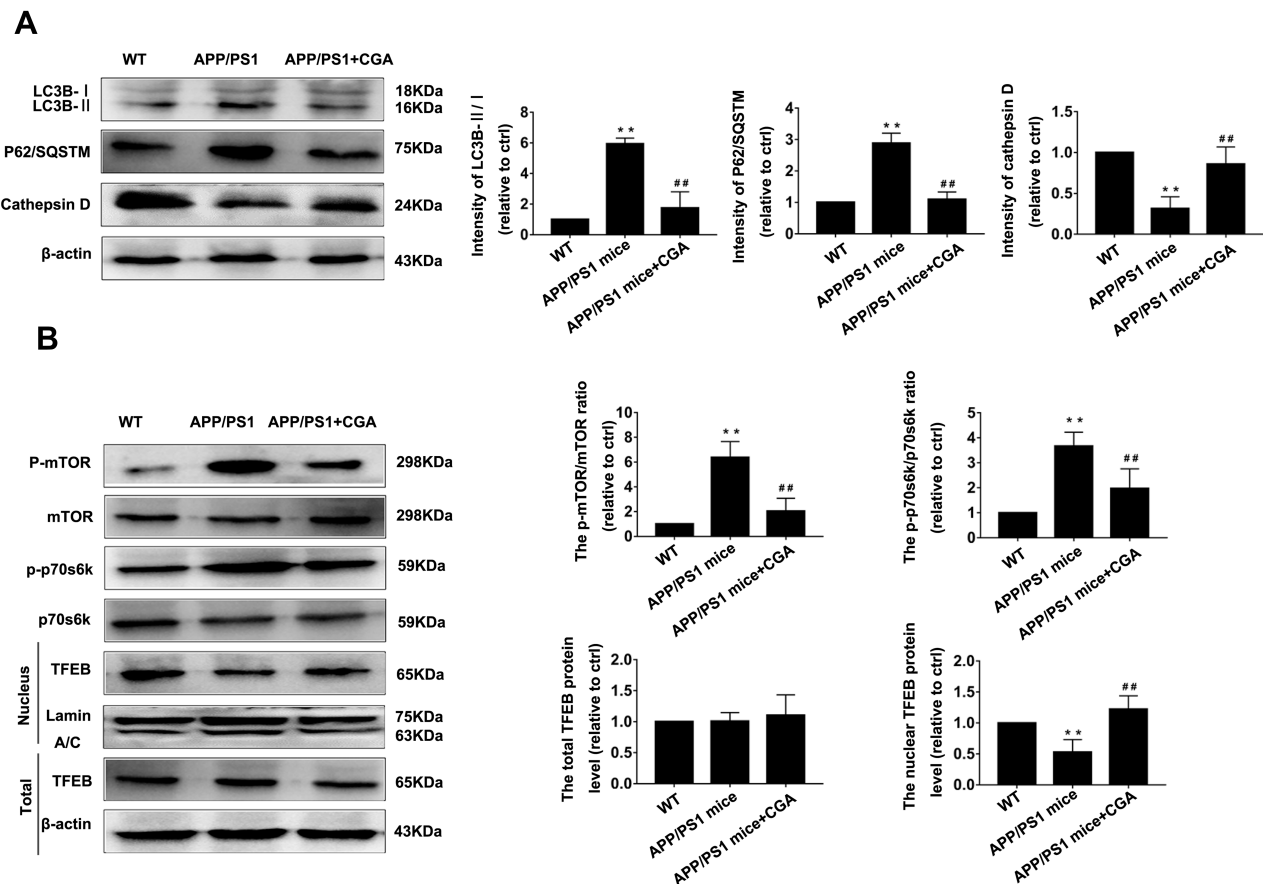
Figure 4 Suppression of autophagy and enhancement of lysosomal function by CGA in APP/PS1 mice.

Notes: (**A**) Representative Western blot imagines of LC3B-II/LC3B-I (16/18 KDa), p62/SQSTM (75 KDa), and cathepsin D (24 KDa) in the brains of APP/PS1 mice (left panel). β-actin (43 KDa) was used as a control for protein loading. The right panel shows the relative optical density values of LC3B-II/LC3B-I, p62/SQSTM, and cathepsin D between the experimental groups. (**B**) Representative Western blot imagines of mTOR (298 KDa), p-mTOR (298 KDa), p70s6k (59KDA) and p-p70s6k (59KDA) in the brains of APP/PS1 mice, and representative Western blot imagines of TFEB (65 KDa) indicating nuclear protein and total protein (left panel); lamin A/C (74/63 KDa) or β-actin (43 KDa) was used as a control for protein loading. The right panel shows the relative optical density values of mTOR and p-mTOR between the experimental groups and the relative optical density values of TFEB between the experimental groups. Data are expressed as the mean ± s.e.m for eight samples per treatment group. **P<0.01 compared with the WT group; ##P<0.01 compared with the APP/PS1 group.

Suppression of Autophagy and Enhancement of Lysosomal Function by CGA in APP/PS1 Mice

To recapitulate the observation that CGA could inhibit Aβ$_{25-35}$-induced autophagy through enhancement of lysosomal function in vivo, the effects of CGA on autophagy and lysosomal function in APP/PS1 mice were examined. Consistent with the in vitro data, the protein levels of LC3B-II/LC3B-I and p62/SQSTM in the brain of APP/PS1 mice were significantly increased compared with those in WT mice (P<0.01, Figure 4A). As expected, LC3B-II/LC3B-I and p62/SQSTM protein levels in the CGA treatment group were much lower than those in the APP/PS1 mice (P<0.01, Figure 4A), suggesting that CGA could suppress autophagy in the brains of APP/PS1 mice.

Furthermore, cathepsin D protein levels and mTOR/TFEB pathway in brains of mice were evaluated with Western blot analysis. Notably, the expressions of cathepsin D and nuclear TFEB were significantly decreased in APP/PS1 mice (P<0.01, Figure 4A, B), and mTOR, p70s6k was markedly activated in APP/PS1 mice (P<0.01, Figure 4B). Moreover, all of these alterations were effectively reversed by CGA treatment (P<0.01, Figure 4A, B). Collectively, these results suggested that CGA could suppress autophagy and promote lysosomal function in APP/PS1 mice by its likely ability to regulate the mTOR/TFEB signaling pathway.

Discussion

Our present study examined the effect and the underlying mechanism of CGA in relation to autophagy and its significance to cognitive function in AD. Our data showed

that APP/PS1 mice exhibited cognitive dysfunction and neuron injury in the CA1 hippocampus, and this was accompanied by excessive autophagy and impaired lysosomal function. CGA treatment significantly inhibited $A\beta_{25-35}$-induced autophagy by modulating lysosomal function in SH-SY5Y cells and, thereby attenuated the loss of CA1 neurons and cognitive defects in APP/PS1 mice. Moreover, the present study also indicated that CGA could suppress the excessive autophagy and augmented cognitive function in APP/PS1 mice by likely modulation of the mTOR/TFEB signaling pathway.

Natural polyphenols, such as curcumin, resveratrol, and epigallocatechin-3-gallate (EGCG), have been proposed as novel therapeutics for AD treatment.[24–26] Chlorogenic acid (CGA) is a polyphenolic metabolite mainly extracted from honeysuckle, green tea, coffee beans,and sunflower.[13] In addition to its strong antioxidative characteristics as a free radical scavenger, CGA has been shown to have a variety pharmacological functions in relation to central nervous system disorders,[14–16] especially in preventing the cognitive deficits of AD.[17] Accumulating evidences have shown that CGA can promote neuronal differentiation[27] and inhibit $A\beta$ plaque deposition by reducing $A\beta$ plaque production and increasing disaggregation of $A\beta$ both in vitro and in vivo.[17,28] Consistent with these previous studies, this current study demonstrated that CGA treatment at a dose of 40 mg/kg by gavage administration effectively prevented cognitive deficits and $A\beta$ plaque deposition in APP/PS1 mice. Considering that the hippocampal CA1 region is one of the most prone areas to atrophy in patients with AD,[29] we also investigated the influence of CGA on neuron cell loss in the CA1 of the hippocampus in APP/PS1 mice and $A\beta_{25-35}$-induced neuronal damage in SH-SY5Y cells. H&E staining and electron micrograph imaging indicated that the decreased cell numbers among the CA1 hippocampal neurons and impaired neuronal ultra-structures were significantly relieved with CGA treatment.

Autophagy, a major pathway for organelle and protein turnover enabled by lysosomal degradative processes, has been generally accepted as a major pathway of neuronal cell destruction and $A\beta$-protein aggregation in AD.[30] However, accumulated data indicate that excessive activation of autophagy is involved in facilitating the production of intracellular $A\beta$ and neuron injuries in AD.[23,31] Consistent with our previous finding that $A\beta_{25-35}$ impairs spatial memory with increased beclin1 and LC3B-II/LC3B-I levels in mice,[23] excessive activation of autophagy with increased LC3B-II/LC3B-I and p62/SQSTM1 expression was observed in the brains of APP/PS1 mice and $A\beta_{25-35}$-

exposed SH-SY5Y cells, while CGA treatment effectively inhibited this excessive activation of autophagy. Since the generation of the autophagosome is mediated by a series of critical autophagy-related (ATG) proteins, such as beclin1 and Atg5, the protein levels of beclin1 and Atg5 in $A\beta_{25-35}$-exposed SH-SY5Y cells were observed, and it was found that CGA inhibited autophagosome generation, as indicated by a significant decrease in $A\beta_{25-35}$-induced up-regulation of beclin1 and Atg5. Moreover, a significant increase in autolysosome following CGA treatment suggests that an enhanced autophagy flux also contributed to activation of autophagy in $A\beta_{25-35}$-exposed SH-SY5Y cells.

Multiple studies have shown that mTOR plays an essential role in the inhibition of autophagy induction.[32] mTOR is a highly conserved serine and/or threonine kinase and localizes predominantly in the membranes of lysosomes.[33] In response to environmental changes, activation of mTOR results in phosphorylation of TFEB and suppressed TFEB nuclear translocation, and this is accompanied by lysosomal deficits, indicating that mTOR negatively regulates autophagic flux in AD.[11,12] Our data showed that CGA enhanced autophagic flux in the brains of APP/PS1 mice and $A\beta_{25-35}$-exposed SH-SY5Y cells via the regulation of mTOR/TFEB signaling, as evidenced by elevated protein levels of p-mTOR,p-p70s6k and nuclear TFEB. Since cathepsin D is an aspartyl protease important for lysosomal proteolysis, we further assessed the effect of CGA on cathepsin D expression in the brains of APP/PS1 mice and $A\beta_{25-35}$ - exposed SH-SY5Y cells. As expected, cathepsin D protein expression was significantly increased after CGA treatment, which was consistent with the LysoTracker result indicating that CGA could significantly increase the LysoTracker fluorescence.

It is generally known that TFEB nuclear translocation binds specifically to a 10-bp motif (GTCACGTGAC) in the promoter regions of many genes that encode lysosomal and autophagic proteins.[34] But in this study, CGA promoted TFEB translocation and inhibited ATG5 and beclin1 expression. Based on recent studies, the role of TFEB in neurodegenerative disease may possibly be two-sided. On the one hand, TFEB inhibition or cytoplasmic sequestration could result in deficiency in the Autophagy–lysosomal pathway, worsen the accumulation of pathologic aggregates. On the other hand, TFEB could be upregulated in response to lysosomal stress resulting from a preexisting insult such as mutation or dysfunction in other components of the Autophagy–lysosomal pathway; however, it remains unable to compensate for increasing disease pathology. In both scenarios, the net result is TFEB

insufficiency and should therefore be offset by enhanced TFEB activity.[35] New research shows that different mechanisms of TFEB activation may operate to modulate the transcriptional regulation of the cellular adaptation to stress depending on the cell type and/or the nature of the stimulus.[36] Therefore, TFEB nuclear translocation does not necessarily promote autophagy generation, and there are many other factors that affect autophagy. Other studies have shown that mTOR promotes anabolic metabolism and inhibits autophagy induction. This contradicts with this study. But Some previous studies have shown that the mRNA levels of Beclin1 and mTOR are increased by $A\beta_{25-35}$.[37] Moreover, Western blot assays show that $A\beta_{25-35}$ increases the levels of Beclin-1 protein and p-mTOR/mTOR in SH-SY5Y cells. These data confirm the upregulation of autophagy in the $A\beta_{25-35}$-induced SH-SY5Y cell line. Besides, TNF-α increased the phosphorylation mTOR and the expression of Atg5, Beclin-1 and LC3-II/LC3-I at the same time.[38] This is consistent with the trend of protein expression level in this study. Therefore, increased phosphorylated mTOR levels do not necessarily inhibit ATG5 and Beclin1 protein levels. The complex pattern of upstream pathways that converge on mTOR suggests that this complex acts as a node, converting multiple signals into autophagosome formation.[39] mTOR is not the only target to regulate ATG5 and Beclin1, the expression of autophagy protein is a complex process, which is affected by many factors such as:

1) Low intracellular calcium levels downregulated the cleavage activity of Calpain 1, increased the level of Atg5 and Atg12-Atg5 and ultimately upregulated autophagy. Thus, ATG5 levels can be regulated via Calpain 1 cleavage, which has a marked influence on autophagy.[40] 2) Similarly, microRNA miR181a interacts with miRNA response element in the 3′ untranslated region (UTR) of Atg5, which inhibits its transcription. Overexpression of miR181a significantly attenuates Atg5 mRNA and protein levels, resulting autophagy inhibition.[40] 3) RACK1, which was an interaction partner of Atg5 and a novel regulator of Autophagy.[40,41]

However, this paper also has some disadvantages, autophagy was not observed in The TEM images. This does not mean that autophagy did not occur. We can only speculate on the reasons for this change. It is speculated that the reason may be that autophagy entered the degradation stage at the time we detected. But we can see obvious neuronal damage.

Conclusion

Altogether, these results demonstrated that CGA could exert a neuroprotective effect against neuronal injury by facilitating autophagic flux in APP/PS1 mice.

Disclosure

The authors report no conflicts of interest in this work.

References

1. Huber CM, Yee C, May T, et al. Cognitive decline in preclinical alzheimer's disease: amyloid-beta versus tauopathy. *J Alzheimers Dis*. 2018;61(1):265–281. doi:10.3233/JAD-170490
2. Querfurth HW, LaFerla FM. Alzheimer's disease. *N Engl J Med*. 2010;362(4):329–344. doi:10.1056/NEJMra0909142
3. Selkoe DJ, Hardy J. The amyloid hypothesis of alzheimer's disease at 25 years. *EMBO Mol Med*. 2016;8(6):595–608. doi:10.15252/emmm.201606210
4. Sevigny J, Chiao P, Bussière T, et al. The antibody aducanumab reduces Aβ plaques in Alzheimer's disease. *Nature*. 2016;537 (7618):50–56. doi:10.1038/nature19323
5. Menzies FM, Fleming A, Rubinsztein DC. Compromised autophagy and neurodegenerative diseases. *Nat Rev Neurosci*. 2015;16 (6):345–357. doi:10.1038/nrn3961
6. Luo R, Su LY, Li G, et al. Activation of PPARA-mediated autophagy reduces Alzheimer disease-like pathology and cognitive decline in a murine model. *Autophagy*. 2019;16;1–18.
7. Wani A, Gupta M, Ahmad M, et al. Alborixin clears amyloid-β by inducing autophagy through PTEN-mediated inhibition of the AKT pathway. *Autophagy*. 2019;15;1–19.
8. Settembre C, Di Malta C, Polito VA, et al. TFEB links autophagy to lysosomal biogenesis. *Science*. 2011;332(6036):1429–1433. doi:10.1126/science.1204592
9. Yamamoto F, Taniguchi K, Mamada N, et al. TFEB-mediated enhancement of the autophagy-lysosomal pathway dually modulates the process of amyloid β-protein generation in neurons. *Neuroscience*. 2019;402:11–22. doi:10.1016/j.neuroscience.2019.01.010
10. Settembre C, Fraldi A, Medina DL, et al. Signals from the lysosome: a control centre for cellular clearance and energy metabolism. *Nat Rev Mol Cell Biol*. 2013;14(5):283–296. doi:10.1038/nrm3565
11. Song HL, Demirev AV, Kim NY, et al. Ouabain activates transcription factor EB and exerts neuroprotection in models of alzheimer's disease. *Mol Cell Neurosci*. 2019;95:13–24. doi:10.1016/j.mcn.2018.12.007
12. Cortes CJ, La Spada AR. TFEB dysregulation as a driver of autophagy dysfunction in neurodegenerative disease: molecular mechanisms, cellular processes, and emerging therapeutic opportunities. *Neurobiol Dis*. 2019;122:83–93. doi:10.1016/j.nbd.2018.05.012
13. Naveed M, Hejazi V, Abbas M, et al. Chlorogenic acid (CGA): a pharmacological review and call for further research. *Biomed Pharmacother*. 2018;97:67–74. doi:10.1016/j.biopha.2017.10.064
14. Song J, Zhou N, Ma W, et al. Modulation of gut microbiota by chlorogenic acid pretreatment on rats with adrenocorticotropic hormone induced depression-like behavior. *Food Funct*. 2019;10 (5):2947–2957. doi:10.1039/c8fo02599a
15. Rebai O, Amri M. Chlorogenic acid prevents AMPA-mediated excitotoxicity in optic nerve oligodendrocytes through a PKC and caspase-dependent pathways. *Neurotox Res*. 2018;34(3):559–573. doi:10.1007/s12640-018-9911-5

16. Fang SQ, Wang YT, Wei JX, et al. Beneficial effects of chlorogenic acid on alcohol-induced damage in PC12 cells. *Biomed Pharmacother*. 2016;79:254–262. doi:10.1016/j.biopha.2016.02.018

17. Ishida K, Yamamoto M, Misawa K, et al. Coffee polyphenols prevent cognitive dysfunction and suppress amyloid β plaques in APP/PS2 transgenic mouse. *Neurosci Res*. 2019;pii: S0168-0102(18)30575-3.

18. Domitrović R, Cvijanović O, Šušnić V, et al. Renoprotective mechanisms of chlorogenic acid in cisplatin-induced kidney injury. *Toxicology*. 2014;324:98–107. doi:10.1016/j.tox.2014.07.004

19. Yan H, Gao YQ, Zhang Y, et al. Chlorogenic acid alleviates autophagy and insulin resistance by suppressing JNK pathway in a rat model of nonalcoholic fatty liver disease. *J Biosci*. 2018;43 (2):287–294. doi:10.1007/s12038-018-9746-5

20. Weng J, Weng J, Ren L, et al. Interactions between gold nanoparticles and amyloidβ 25-35 peptide. *Nanobiotechnol Iet*. 2014;8(4):295–303. doi:10.1049/iet-nbt.2013.0071

21. Ohkawara T, Takeda H, Nishihira J.Protective effect of chlorogenic acid on the inflammatory damage of pancreas and lung in mice with, l -arginine-induced pancreatitis[J]. *Life Sci*.2017;190:91–96. doi:10.1016/j.lfs.2017.09.015

22. Fu W, Dai Y, Ma T, et al. Tongluo Xingnao effervescent tablet reverses memory deficit and reduces plaque load in APPswe/PS1dE9 mice. *Exp Ther Med*. 2018;15(4):4005–4013. doi:10.3892/etm.2018.5897

23. Zhu J, Chen X, Song Y, et al. Deficit of RACK1 contribute to the spatial memory impairment via up regulating BECLIN1 to induce autophagy. *Life Sci*. 2016;151:115–121. doi:10.1016/j.lfs.2016.02.014

24. Jabir NR, Khan FR, Tabrez S. Cholinesterase targeting by polyphenols: a therapeutic approach for the treatment of Alzheimer's disease. *CNS Neurosci Ther*. 2018;24(9):753–762. doi:10.1111/cns.12971

25. Nuzzo D, Presti G, Picone P, et al. Effects of the Aphanizomenon flos-aquae Extract (Klamin®) on a neurodegeneration cellular Model. *Oxid Med Cell Longev*. 2018;2018:1–14. doi:10.1155/2018/9089016

26. Nuzzo D, Amato A, Picone P, et al. A natural dietary supplement with a combination of nutrients prevents neurodegeneration induced by a high fat diet in mice.[J]. *Nutrients*. 2018;10(9):1130. doi:10.3390/nu10091130

27. Ito H, Sun XL, Watanabe M, et al. Chlorogenic acid and its metabolite m-coumaric acid evoke neurite outgrowth in hippocampal neuronal cells. *Biosci Biotechnol Biochem*. 2008;72(3):885–888. doi:10.1271/bbb.70670

28. Miyamae Y, Kurisu M, Murakami K, et al. Protective effects of caffeoylquinic acids on the aggregation and neurotoxicity of the 42-residue amyloid β-protein. *Bioorg Med Chem*. 2012;20 (19):5844–5849. doi:10.1016/j.bmc.2012.08.001

29. Blanken AE, Hurtz S, Zarow C, et al. Associations between hippocampal morphometry and neuropathologic markers of Alzheimer's disease using 7 T MRI. *Neuroimage Clin*. 2017;15:56–61. doi:10.1016/j.nicl.2017.04.020

30. Orr ME, Oddo S. Autophagic/lysosomal dysfunction in Alzheimer's disease. *Alzheimers Res Ther*. 2013;5(5):53. doi:10.1186/alzrt217

31. Tung YT, Wang BJ, Hu MK, et al. Autophagy: a double-edged sword in Alzheimer's disease. *J Biosci*. 2012;37(1):157–165. doi:10.1007/s12038-011-9176-0

32. Laplante M, Sabatini DM. mTOR signaling in growth control and disease. *Cell*. 2012;149(2):274–293. doi:10.1016/j.cell.2012.03.017

33. Sancak Y, Bar-Peled L, Zoncu R, et al. Ragulator-Rag complex targets mTORC1 to the lysosomal surface and is necessary for its activation by amino acids. *Cell*. 2010;141(2):290–303. doi:10.1016/j.cell.2010.02.024

34. Nezich CL, Wang C, Fogel AI, et al. MiT/TFE transcription factors are activated during mitophagy downstream of Parkin and Atg5[J]. *J Cell Biol*. 2015;210(3):435–450. doi:10.1083/jcb.201501002

35. Martini-Stoica H, Xu Y, Ballabio A, et al. The autophagy–lysosomal pathway in neurodegeneration: a TFEB perspective[J]. *Trends Neurosci*. 2016;39:221–234.

36. Brady OA, Martina, José A, Puertollano R. Emerging roles for TFEB in the immune response and inflammation[J]. *Autophagy*. 2017;14;1–9.

37. Wang L, Jin G, yu H, et al. Protective effect of Tenuifolin against Alzheimer's disease. [J]. *Neurosci Lett*. 2019;705:195–201.

38. Deng H, Zheng M, Hu Z, Zeng X, Kuang N, Fu Y. Effects of daphnetin on the autophagy signaling pathway of fibroblast-like synoviocytes in rats with collagen-induced arthritis (CIA) induced by TNF-alpha. *Cytokine*. 2019;127:154952. doi:10.1016/j.cyto.2019.154952

39. Zachari M1, Ganley IG2. The mammalian ULK1 complex and autophagy initiation[J]. *Essays Biochem*. 2017;61(6):585–596. doi:10.1042/EBC20170021

40. Ye X, Xu-Jie Z, Zhang H. immunology, EXPLORING THE ROLE OF AUTOPHAGY-RELATED GEne 5(ATG5) yields important insights into autophagy in autoimmune/autoinflammatory diseases. *Front Immunol*. 2018;9:2334. doi:10.3389/fimmu.2018.02334

41. Erbil S, Oral O, Mitou G, et al. RACK1 is an interaction partner of ATG5 and a novel regulator of autophagy[J]. *J Biol Chem*. 2016;291 (32):16753–16765. doi:10.1074/jbc.M115.708081